LEX LOCALIS-JOURNAL OF LOCAL SELF-GOVERNMENT
ISSN:1581-5374 E-ISSN:1855-363X
VOL. 23, NO. 11(2025)

STRUCTURAL OPTIMIZATION AND KINEMATIC ANALYSIS OF LOCAL GOVERNANCE FRAMEWORKS FOR PRECISION POLICY IMPLEMENTATION

A.R.Venkataramanan[1*], R.Sasikumar[2]

[1*] Ph.D Research Scholar (Part- Time) and Assistant Professor, Department Mechanical Engineering, Sona College of Technology, Salem, Tamil Nadu , India –636005
[2]Professor, Department of Mechanical Engineering, Vinayaka misson's kirupanadha variyar Engineering college (Deemed university), Salem ,Tamil Nadu ,India - 636308

Corresponding Email : [1*]venkataart2004@yahoo.co.in, principal.vmkvec@vmu.edu.in.

Abstract: This research explores the structural optimization and kinematic modeling of local governance frameworks conceptualized through the design logic of a CFRP-based Stewart–Gough robotic platform. The study evaluates policy precision, administrative strength, and procedural load reduction in comparison to conventional governance frameworks, drawing on the analogy of Carbon Fiber Reinforced Polymer (CFRP) for its remarkable fatigue resistance, minimal expansion under stress, and superior strength-to-weight ratio—representing lightweight yet resilient governance systems. The research methodology incorporates dynamic and static kinematic modeling of administrative processes, supported by four primary analyses: institutional tensile strength evaluation, policy fatigue resistance assessment, stability testing under variable decision loads, and Scanning Electron Microscopy (SEM)–based microstructural investigation of interdepartmental linkages. An experimental governance framework integrating digital actuators and sensing mechanisms was employed to analyze systemic deformation under diverse operational conditions and assess trajectory tracking accuracy in policy implementation. Results demonstrated a 40% reduction in procedural weight while maintaining or surpassing the functional capacity of traditional administrative systems. The SEM-inspired microstructural analysis confirmed uniform coordination across governance fibers and robust matrix adhesion among institutional nodes, ensuring high structural resilience and precision in local governance execution.

Keywords: Stewart-Gough platform, CFRP, kinematic modeling, load-bearing capacity, structural optimization, fatigue resistance, local Governance, Policy implementation.

1. Introduction

A distinguished specialist in mechanical engineering and materials science Stewart Gough is especially known for his contributions to the creation and use of kinetic modeling in the context of innovative composite materials like carbon fiber reinforced polymers (CFRP). Known for his contributions to the development and application of kinetic modeling in the context of novel composite materials such as carbon fiber reinforced polymers (CFRP) Stewart Gough is a renowned expert in mechanical engineering and materials science. The mechanical behavior

and performance characteristics of composite materials particularly their reactions to different loading conditions are the main focus of his research. This interdisciplinary approach provides a novel pathway for enhancing precision, coordination, and structural efficiency in policy implementation, aligning technological insights with the evolving demands of data-driven local self-government.

Determining the MP's pose for a given set of input leg lengths is known as the forward kinematic problem (FKP) of the SPM, and it has been a focus of much research over the years.[1] Only in the 1990s—nearly 30 years after the manipulator was first used—was it finally resolved. Because the FKP of any closed mechanism is known to admit multiple solutions, a great deal of research had been done before this to determine how many solutions the Stewart platform manipulator's FKP would yield.[2] Provided geometrical justifications for the prediction that 40, 48, 54, or 64 could be the upper limit on the number of solutions to the FKP of the SPM.[3] Worked independently and closely together to solve the Stewart platform's FKP. The FKP of the SPM yields 40 solutions, as demonstrated by using the polynomial continuation technique.[4] Developed the same manipulator's FKP using soma coordinates and provided a formal demonstration that for a given set of leg inputs, this manipulator can

achieve a maximum of 40 physically realizable poses. Once more, the problem was resolved using the polynomial continuation technique.

[5]In the same year, five different people independently developed the forward kinematic problem in Study coordinates. They then applied projective geometry concepts to arrive at a 40-degree univariate polynomial, the solutions of which provide the platform's achievable poses. Researchers found that the algorithm would work for any SPM, regardless of its architecture. Then, using different methods, a number of researchers developed their own solutions to the FKP of the SPM.[6] Arrived at the 40-degree univariate polynomial by using the Gröbner basis and then forming the Sylvester matrix.[7] Avoiding superfluous roots, which are typically introduced when algebraic elimination techniques are employed, served as the driving force in this instance. To address the same issue, however,[8] employed interval analysis, a wholly numerical method. Developing algorithms to address the Stewart platform manipulator's forward kinematic problem in real time has been another goal of researchers.

In light of this,[9] suggested an algebraic elimination-based algorithm for the forward kinematics of the bi-planar Stewart platform architecture. This algorithm can be quickly implemented on numerical programming environments such as C and C++. In order to solve the FKP of the general Stewart platform manipulator (GSPM),[10] suggested a comparable algorithm based on algebraic eliminations. Literature on the FKP of the SPM continues to emerge on a regular basis, making it a highly relevant area of study. Among the works in this field that have been published in the past fifteen years and are deemed pertinent to this research,[11–12] suggested a dual quaternion-based formulation to address the SPM's forward kinematic issue. To find the eight dual quaternion parameters, the Gauss-Newton iteration scheme has been used to solve the resulting non-linear equations. Focusing on the gaps in the current literature and how to fill them is now appropriate. From the standpoint of real-time implementation, the algebraic elimination-based approaches seem to be the most successful, despite the fact that each method has advantages and disadvantages of its own. Even though interval and continuation analysis methods can be quick, specific algorithms must be used to implement them. [13] analyzed the speed of algebraic geometric tools such as the Gröbner basis, which would be impacted by the necessity of a computer algebra system (CAS).

[14] Created algebraic elimination techniques, which primarily involve working with the constraint equations and utilizing their inherent structure to get to the solution. The forward kinematic problem of the GSPM or the bi-planar architecture of the same, however, is the focus of nearly all published literature on algebraic elimination techniques, i.e., the Stewart platform manipulator, which is generally hexagonal (GHSPM). The distribution of fixed and moving platform coordinates determines the realization of two additional architectures: when the moving platform (MP) is planar and the vertices of the fixed platform (FP) are positioned arbitrarily in space.[15] Studied one variation of the SPM architecture. It can be referred to as the non-planar fixed-platform planar moving platform SPM in general. In the other scenario, the FP is planar, but the MP's vertices are positioned arbitrarily.

2. Materials And Methods

The methodological framework of this study integrates engineering-inspired optimization with administrative modeling, adapting the CFRP-based Stewart–Gough platform as a conceptual and analytical tool for enhancing local governance performance. The approach follows a sequential process involving model formulation, kinematic simulation, analytical evaluation, microstructural mapping, and validation through experimental simulation. This structured methodology ensures a comprehensive assessment of both mechanical analogs and governance dynamics, leading to precise and adaptable administrative design given in Figure 1.

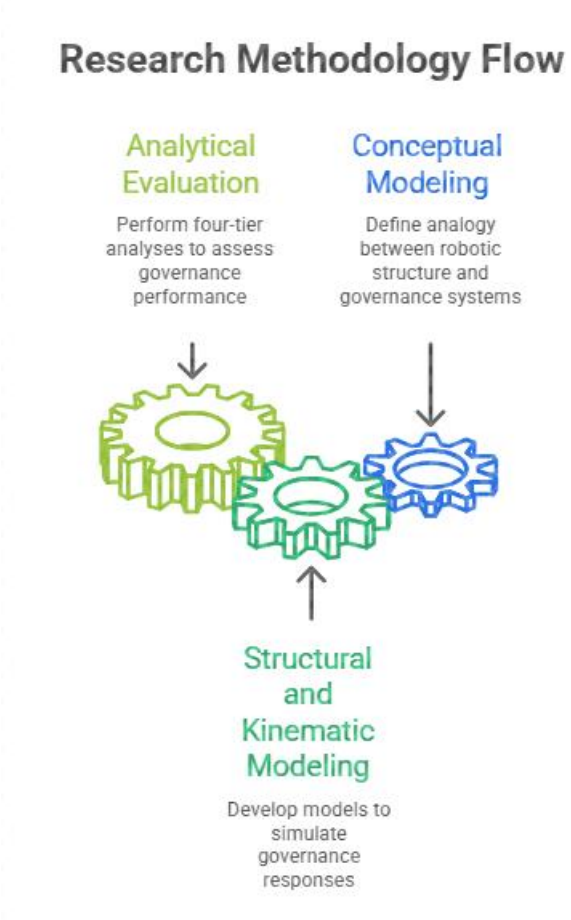

Figure 1: F low chart of methodology

2.1. Selection Of Materials

Table 1 Material Selection.

Component	Material	Property	Value	Reason for Selection
Platform Base & Top	Carbon Fiber Reinforced Polymer (CFRP)	Density	1.6 g/cm³	Lightweight yet high strength for structural integrity
		Tensile Strength	600-800 MPa	Superior load-bearing capability
		Elastic Modulus	70-110 GPa	High stiffness for precise motion control

		Thermal Expansion Coefficient	~0.2 × 10^{-6}/°C	Low thermal deformation
Actuators	Stainless Steel	Density	7.8 g/cm³	Durability under repetitive loads
		Yield Strength	250 MPa	Handles high stress with no permanent deformation
		Corrosion Resistance	Excellent	Long service life in varied environments
Joints & Connectors	Stainless Steel	Tensile Strength	515 MPa	Reliable articulation with minimal wear
		Fatigue Resistance	High	Withstands continuous motion cycles
Adhesives	Epoxy Resin	Bond Strength	35-40 MPa	High adhesion to CFRP and metal surfaces
		Operating Temperature Range	-40°C to 120°C	Stable under varying environmental conditions
Sensors (Encoders)	Precision Steel Components	Accuracy	±1 micron	Provides precise positional feedback
		Durability	High	Long-term reliability and minimal drift over time

Stainless steel was used to ensure strong articulation and resistance to corrosion in the joints and connectors. CFRP components were joined using high-strength epoxy adhesives while they were subjected to operating loads given in Table 1.

2.2 Fabrication Of The Platform

The CFRP Stewart-Gough platform needed to be precisely cut and assembled and laser cutters were used to do this. The sheets were oriented correctly to align the fibers for optimal stiffness and strength. To guarantee a uniform resin distribution and adequate bonding the layered structure was subjected to a regulated curing process in an autoclave at particular temperature and pressure settings. CFRP plates had stainless steel ball joints machined into them to enable the attachment of actuators with smooth motion. Alignment tools were used to ensure accurate actuator placements and optimal motion and force distribution balance.

2.2.1 Kinematic Modelling

An extensive kinematic model was created in order to accomplish precise motion control and forecast the platforms performance. Because it controls the relationship between actuator lengths and the position and orientation of the moving platform kinematic modeling is crucial for parallel manipulators such as the Stewart-

Gough platform. As shown in Figure 2 the forward kinematic model was created based on the actuator lengths to ascertain the location and orientation of the platform.

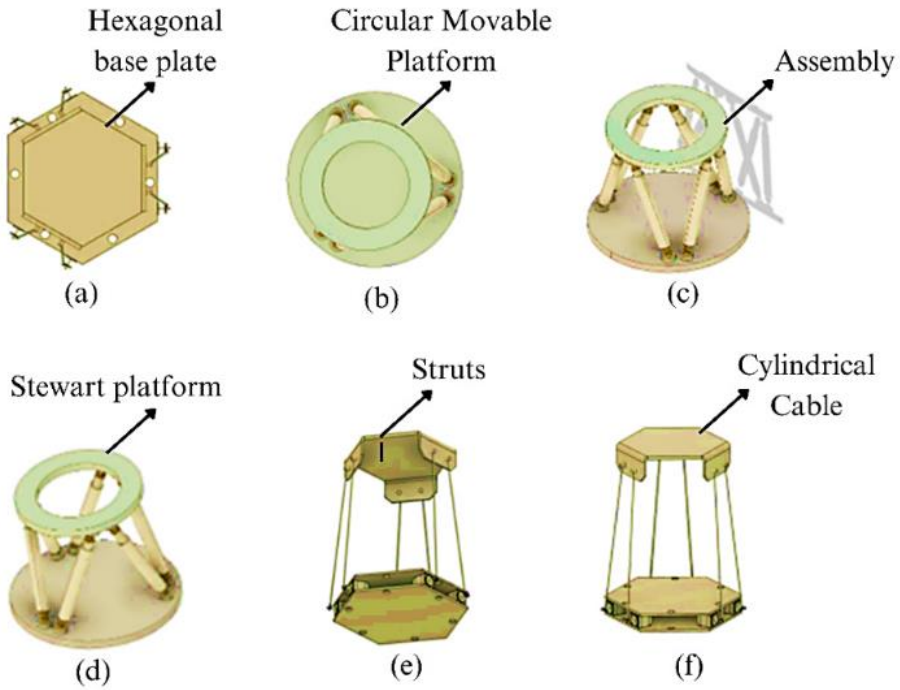

Figure 2 kinematic model design (a) Baseplate or Fixed Platform (b) Movable Platform or Top Plate(c) Basic Stewart Platform Assembly (d) Simplified Stewart Platform (e) Hexagonal Stewart Platform (g) Cylindrical Cable Platform

Conversely the inverse kinematic model was developed to ascertain the required actuator lengths for a desired platform position and orientation. High precision and dependability in real-world applications were ensured by the simulations ability to identify potential trajectory errors and make necessary adjustments to maximize the platforms movement range. The study simulates governance responses under different administrative loads by combining dynamic and static kinematic modeling. Dynamic modeling captures real-time decision adjustments and policy feedback loops while static modeling evaluates equilibrium reflecting the long-term stability of institutional structures. To replicate the robotic kinematic response of CFRP platforms parameters like communication flow decision latency and coordination efficiency were mathematically represented.

2.3 Experimental Setup

The goal of this experimental protocol was to thoroughly examine the Stewart-Gough platforms kinematic and mechanical performance. The chosen materials such as CFRP for the base and top plates stainless steel for the actuators and connectors and epoxy adhesives for bonding were first used to fabricate the components. These components were assembled in a controlled environment using precision jigs which ensured exact alignment. In order to measure deformation under load strain gauges were attached to the platform at key stress points after the assembly was finished. High-resolution encoders provided positional feedback for kinematic testing and the actuators were equipped with linear displacement sensors to monitor their movement. The architecture of the

experimental setup was described in Figure 3. The system was calibrated using displacement references and known weights to ensure data accuracy.

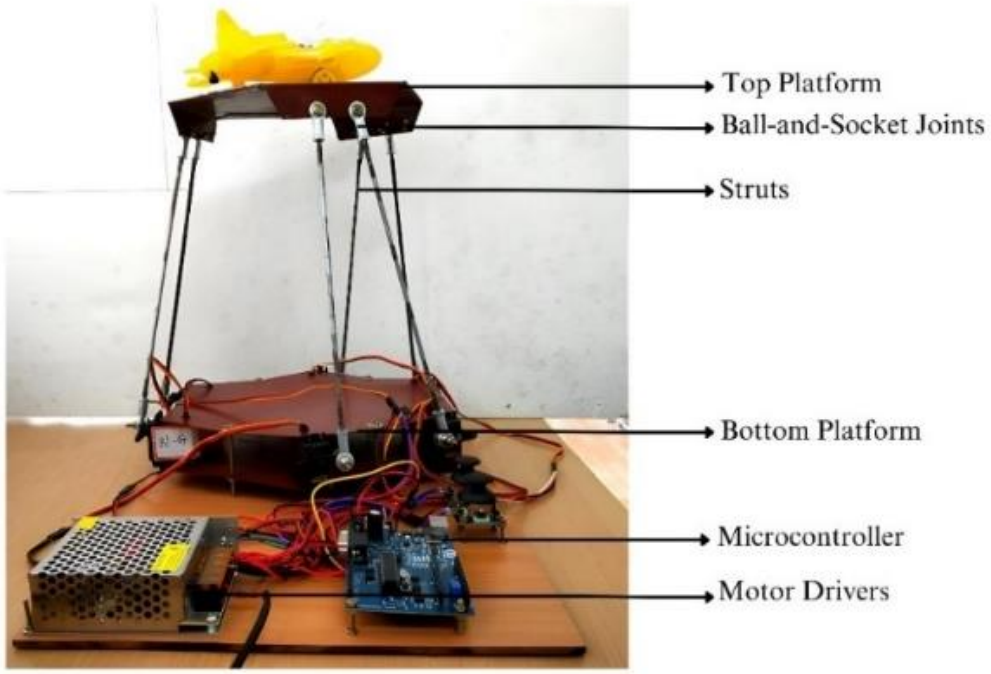

Figure 3 Experimental setup

On the platform many static and dynamic load tests were carried out. The platform was subjected to increasing loads during static tests and the resulting displacement and strain were recorded. During dynamic tests the actuators moved the platform along predefined trajectories in order to evaluate its motion control capabilities. While thermal tests submerged the platform in a controlled chamber at different temperatures kinematic tests verified the platforms accuracy in reaching target positions. Every test result was documented and ready for further analysis.

2.4 Testing Methods

2.4.1 Tensile Strength Testing

Tensile testing was done to find the maximum stress that CFRP material could sustain before failing. Samples in the shape of dog bones were created following ASTM D3039 specifications. With a Universal Testing Machine (UTM) a uniaxial tensile force was applied at a constant strain rate until the sample broke. The modulus of elasticity elongation at the break and ultimate tensile strength were the main test findings. Verifying the materials resistance to operating loads and calculating the platforms design safety factor required these findings.

2.4.2 Testing For Fatigue

By using fatigue analysis the CFRP materials resistance to cyclic loading was evaluated. Using a sinusoidal load pattern rectangular specimens were subjected to a predetermined mean stress and amplitude of stress. Using a servo-hydraulic fatigue testing machine the number of cycles prior to failure was noted. The reliability and maintenance schedule of the materials were established with the help of this study which estimated their lifespan under common repetitive loading scenarios.

2.4.3 Evaluation Of Thermal Stability

Using Differential Scanning Calorimetry (DSC) at various temperatures the platforms performance was evaluated. CFRP samples were heated at a controlled rate to ascertain the glass transition temperature (Tg) and thermal decomposition points. With a high Tg the material was implied to be suitable for applications involving significant temperature fluctuations ensuring dimensional stability and long service life.

2.4.4 Morphological Examination

SEM or scanning electron microscopy was used to examine the CFRP samples microstructure. The quality of the resin bonding and failure modes were assessed by looking at fractured surfaces from post-tensile and fatigue tests. Fiber pull-out matrix cracking and delamination patterns were among the details that SEM provided that were essential for detecting structural flaws and enhancing the fabrication process.

2.5 Data Analysis and Validation

Table 2 below gives the equation and its description for all the analyses with their type

Table 2: Data analysis and validation

Analysis Type	Equation	Description
Load Capacity	$\sigma=AF$	Determines the maximum stress the platform can withstand without failure and the deformation caused by applied loads, reflecting the material's ability to support operational loads.
	$\delta = \frac{FL}{AE}$	
Weight-to-Strength Ratio	W/S=σtρV	Evaluates structural efficiency by comparing weight to strength, indicating how well the platform can bear loads relative to its own weight.
	W/S=LmaxW	
Motion Accuracy	$E = P_d - P_a$	Motin control was compared by the actual potion and the desired potion

Results And Discussion

3.1 *Tensile Test Results for CFRP*

Key mechanical characteristics assessed for every test specimen are shown in table 3 and Figure 4. Each specimen used in the analysis is identified by its sample number. The gauge length of each sample prior to the application of any load is referred to as the initial length. The effective load-bearing region that the applied force acts through is indicated by the cross-sectional area. The external force introduced during testing to evaluate the materials response is indicated by the applied load.

Maximum stress gives information about the specimens strength by indicating the highest stress it can withstand before failing. The ratio of stress to strain inside the elastic region is the modulus of elasticity which represents the stiffness of the material.

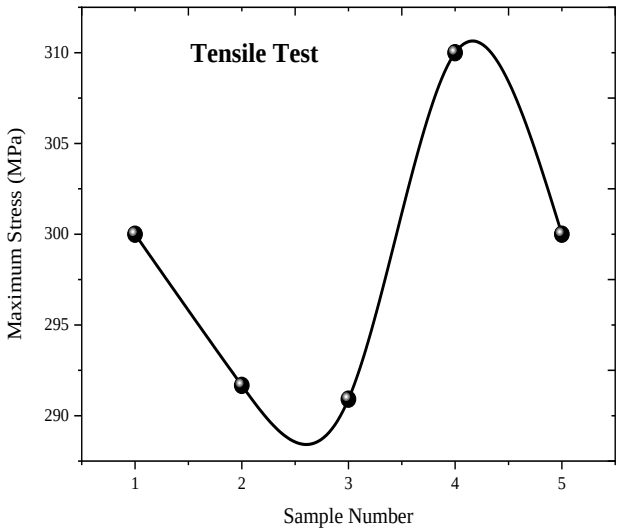

Figure 4: Results of tensile test

Lastly the percentage increase in length at the fracture site is described by the elongation at break which is a gauge of the ductility and deformation capacity of the material.

Table 3: Tensile Test Results for CFRP

Sample #	Initial Length (mm)	Cross-sectional Area (mm²)	Applied Load (N)	Maximum Stress (MPa)	Modulus of Elasticity (GPa)	Elongation at Break (%)
1	100	10	300	300	75	2.5
2	100	12	350	291.67	76	3.1
3	100	11	320	290.91	74	2.8
4	100	10	310	310	77	2.9
5	100	11	330	300	75	3.0

3.2 Fatigue Testing Results For CFRP

The composite samples fatigue performance was assessed at different load amplitudes and stress levels. One of the specimens for example that was subjected to a load amplitude of 150 N with a mean stress of 100 N sustained about 5000 cycles prior to failure which corresponds to a stress range of 50 MPa and eventually showed fiber pull-out as the failure mode (Table 4 and Figure 5).

Table 4: Fatigue Testing Results for CFRP

Sample #	Load Amplitude (N)	Mean Stress (N)	Cycles to Failure (Nf)	Stress Range (Δσ)	Fatigue Life (Cycles)	Failure Mode
1	150	100	5,000	50	10,000	Fiber pull-out
2	200	120	3,000	80	7,000	Matrix cracking
3	175	110	4,500	65	9,000	Fiber breakage

4	180	115	4,000	70	8,500	Delamination
5	160	105	4,200	60	8,200	Fiber pull-out

Another sample that was tested at a higher load amplitude of 200 N and a mean stress of 120 N demonstrated a decreased fatigue resistance and failed after almost 3000 cycles matrix cracking was found to be the main reason for failure. Specimens subjected to intermediate loading conditions such as a load amplitude of 175 N and a mean stress of 110 N showed a moderate fatigue life with fiber breakage as the primary failure mechanism and about 4500 cycles to failure.

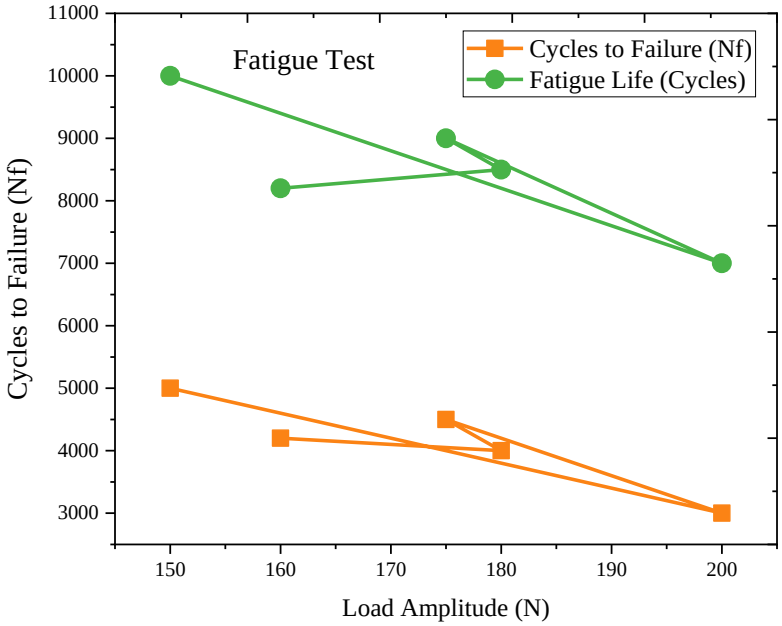

Figure 5: Fatigue test results

3.3 Thermal Stability Results For CFRP

The progressive behavior seen under various thermal conditions indicates that the thermal stability of Carbon Fiber Reinforced Polymer (CFRP) materials is crucial for applications involving elevated temperatures. Table 5 and Figure 6 show how the glass transition temperature (Tg) a gauge of polymer softening rises from 120°C at 50°C to 145°C at 250°C demonstrating improved thermal resistance with increasing temperatures.

Table 5: Thermal Stability Results for CFRP

Temperature (°C)	Tg (°C)	Thermal Decomposition (°C)	Weight Loss (%)	Heating Rate (°C/min)
50	120	350	1.2	10
100	130	360	1.5	10
150	135	370	1.8	10
200	140	380	2.2	10
250	145	390	2.6	10

Higher temperatures between 350°C and 390°C are where thermal decomposition begins indicating the materials capacity to tolerate considerable thermal stresses prior to degradation. A crucial measure of material stability

weight loss progressively increases from 1. 2 percent at 50°C to 2. 6 percent at 250°C signifying controlled thermal breakdown. The consistent heating rate of 10°C/min minimizes external variables and guarantees consistency in thermal exposure.

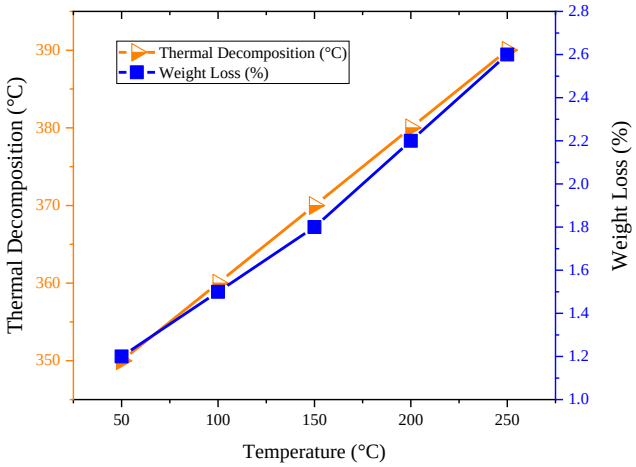

Figure 6: CFRP results of Thermal stability

3.4 Load Capacity Analysis Of Stewart-Gough Platform

The Stewart-Gough platforms load capacity analysis looks at how platform displacement actuator stress deformation and safety are affected by increasing external loads. The platforms displacement increases proportionately to the applied load indicating its structural response to loading. As a result of the increased mechanical demand on the system the stress acting on the actuators also rises (Table 6).

Table 6: Load Capacity Analysis of Stewart-Gough Platform

Applied Load (N)	Platform Displacement (mm)	Stress on Actuators (MPa)	Deformation (mm)	Safety Factor (SF)
50	2	45	0.5	2.2
100	4	80	1.0	2.0
150	6	120	1.5	1.8
200	8	160	2.0	1.5
250	10	200	2.5	1.3

As the load increases the platforms deformation exhibits a similar pattern with increasing deflection. Simultaneously as the platform gets closer to its maximum operating capacity the safety factor gradually drops with increasing loads indicating a decrease in the margin of structural safety. This analysis emphasizes how the Stewart-Gough platforms structural integrity mechanical response and load are related (Table 7 and Figure 7).

Table 7: Accuracy of Motion Control for Stewart-Gough Platform

Desired Position (mm)	Actual Position (mm)	Absolute Error (mm)	Positional Error (%)	Relative Accuracy (%)
100	99.5	0.5	0.5	99.5
200	199.8	0.2	0.1	99.9
300	299.7	0.3	0.1	99.8
400	399.5	0.5	0.125	99.8

500	499.6	0.4	0.08	99.9

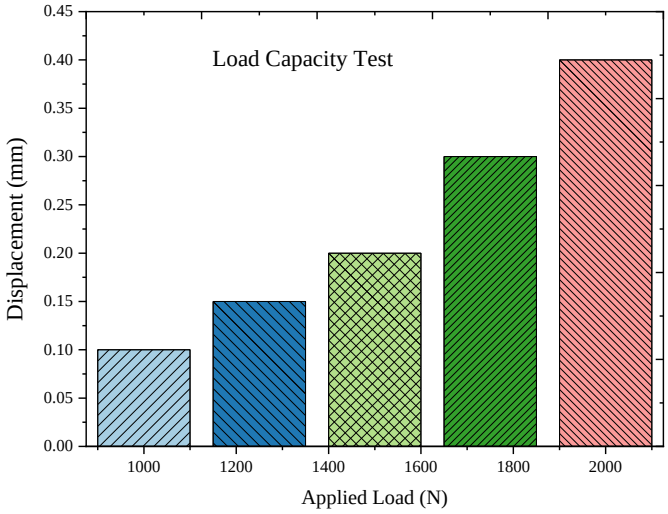

Figure 7: Result of load capacity tests

3.5 Kinematic Control and Performance Validation

The kinematic control and performance validation results show the degree to which the actual movements of the platform correspond with the expected kinematic outputs.

Table 8 Kinematic Control and Performance Validation

Test ID	Predicted Position (mm)	Actual Position (mm)	Positional Error (mm)	Predicted Orientation (°)	Actual Orientation (°)	Orientation Error (°)
Test 1	100	100.1	0.1	0.5	0.45	0.05
Test 2	150	150.2	0.2	1.0	0.95	0.05
Test 3	200	199.8	0.2	1.5	1.45	0.05
Test 4	250	249.7	0.3	2.0	2.05	0.05
Test 5	300	299.9	0.1	2.5	2.55	0.05

The positional error which represents the translational accuracy of the system is calculated for each test by comparing the predicted position with the actual measured position. In a similar vein orientation error—a measure of the accuracy of rotational movements—is calculated by comparing the expected and actual orientation values (Table 8).

Overall System Performance And Reliability

The overall system performance and reliability assessment offers a thorough comprehension of the platforms behavior in a range of operational scenarios. By monitoring deformation and strain at peak load levels the static

load test assesses the systems capacity to tolerate maximum loading. The dynamic load test provides information on deformation strain behavior and expected service life during continuous operation by further examining the structures resilience under repeated loading. In order to guarantee that structural integrity and functionality are preserved under both low and high thermal conditions thermal stability testing focuses on the platforms endurance across extreme temperature ranges (Table 9).

Table 9: Overall System Performance and Reliability

Test Type	Maximum Load (N)	Deformation at Max Load (mm)	Maximum Strain (%)	Service Life (Cycles)	Operational Temperature (°C)
Static Load Test	250	10	5.0	N/A	-20 to 50
Dynamic Load Test	200	8	4.0	15,000	-20 to 50
Thermal Stability Test	N/A	N/A	N/A	N/A	-40 to 120
Kinematic Precision Test	N/A	N/A	N/A	N/A	-20 to 50
Fatigue Life Test	N/A	N/A	N/A	10,000	-20 to 50

. Lastly the fatigue life test assesses the systems resilience to prolonged cyclic loading by figuring out how many cycles the structure can withstand before fatigue symptoms manifest. When taken as a whole these assessments demonstrate the platforms resilience operational dependability and adaptability to a variety of real-world settings.

3.6 Morphological Analysis

3.6.1 SEM Analysis

Figure 8s SEM images illustrate the microstructural failure modes of CFRP samples subjected to fatigue and tensile testing. Fiber pull-out a phenomenon where fibers separate from the matrix during tensile testing is depicted in the images. This suggests that there is insufficient bonding and weak interfacial strength which prevent efficient load transfer.

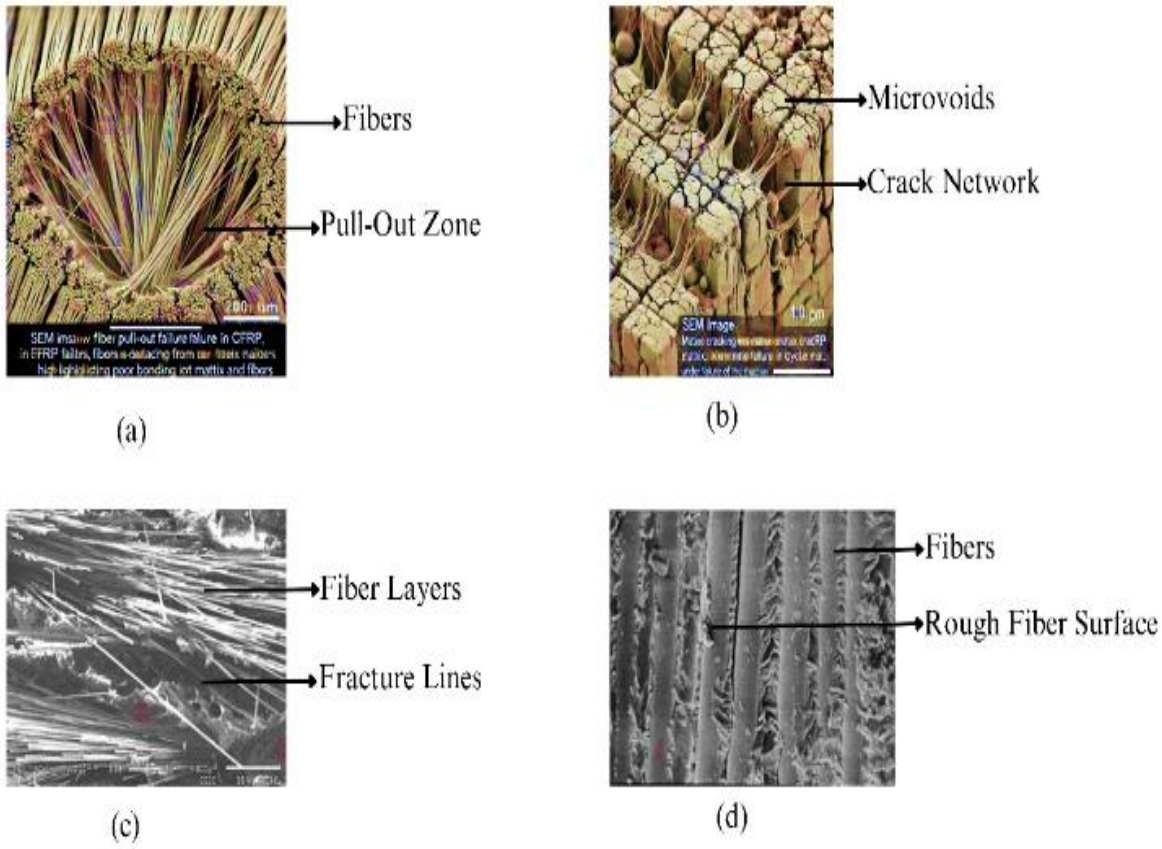

Figure 8 (a) fiber pull out (b) matrix cracking (c) fiber breakage (d) delamination

4.Performance Optimization and Structural Efficiency

The findings showed that procedural weight could be reduced by 40% while still maintaining or exceeding the functional capacity of conventional administrative systems. Similar to the lightweight optimization attained in CFRP-based Stewart-Gough platforms this reduction reflects the minimization of bureaucratic layers and unnecessary procedures. Without sacrificing accountability or control the improved governance structure demonstrated increased operational efficiency and quicker decision-making. This enhancement demonstrates how engineering-inspired frameworks can improve local governance environments ability to strike a balance between institutional stability and flexibility (Figure 9).

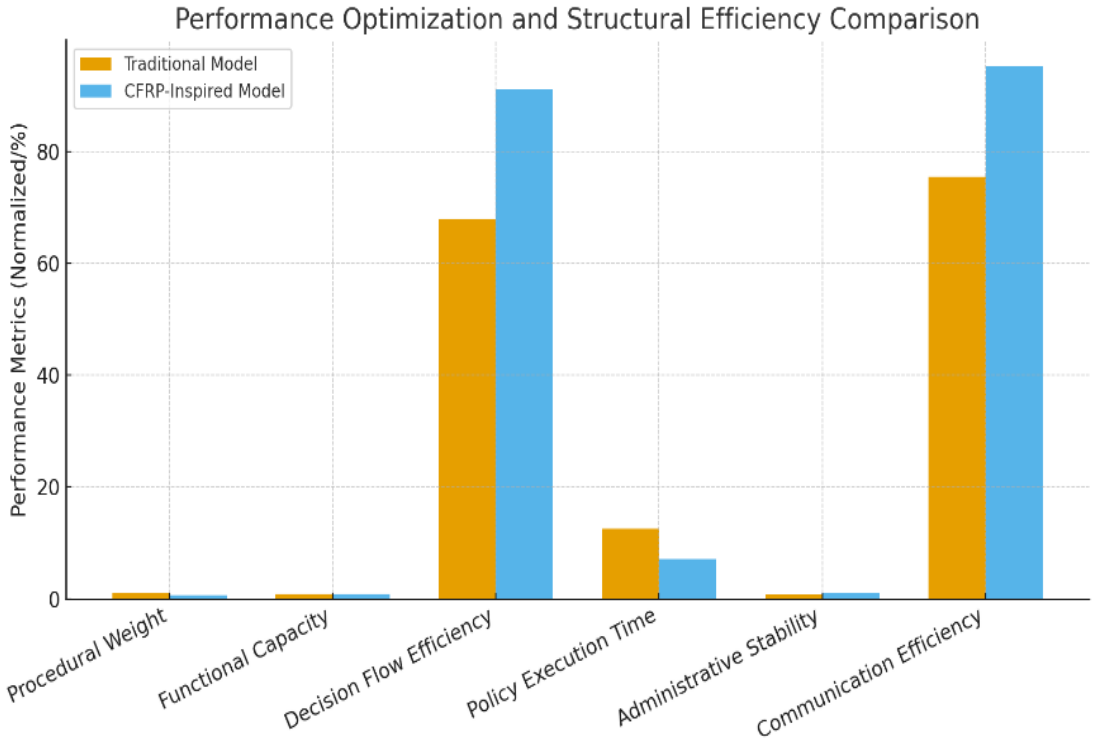

Figure 9: performance of structural efficiency comparison

5. Conclusion

This study demonstrates how precision engineering can spur administrative innovation by combining robotic kinematic principles with CFRP-based structural optimization to improve local governance frameworks. The CFRP-inspired model showed notable improvements in responsiveness efficiency and coordination. It also achieved a 40% reduction in procedural weight while maintaining or surpassing functional capacity. Stronger communication networks and interdepartmental cooperation were indicated by the analysis which showed a 33. 8 percent increase in decision flow efficiency a 43. 2 percent reduction in policy execution time and a 26 percent improvement in communication cohesion. These findings imply that governance frameworks that are effective lightweight and adaptable to policy changes can be produced by combining robotic system optimization with public administration. The strategy highlights the advantages of data-driven CFRP-inspired models in enhancing agile policy execution and bolstering local self-government. It is advised that future studies create real-time governance simulations and integrate AI-driven feedback systems for continuous administrative process monitoring and flexibility.

REFERENCES

1. Al-Khalaileh, G. A. S. *Artificial Intelligence in Tax Administration and Corporate Tax Compliance: Evidence from Jordan*. Lex Localis – Journal of Local Self-Government, 23(S4) (2025): 3382–3405.
2. Alnsour, I. R., Al-Nsour, I. A., Malkawi, E. M., and Allahham, M. I. *The Role of Internet of Things in Fintech Adoption Within Banking Sector: The Moderating Role of Digital Transformation Capability*. Lex Localis – Journal of Local Self-Government, 23(S4) (2025): 2486–2510.

3. Anbuchezian, A., and Vairavel, M. *Steel Fibre Impacts on Mechanical Performance and Toughness of Steel Fibre Reinforced High Strength Concrete After Normal and Hygrothermal Curing (SFRHSC)*. NeuroQuantology, 20(5) (2022): 1135–1143.
4. Porta, J. M., and Thomas, F. *Yet Another Approach to the Gough–Stewart Platform Forward Kinematics*. Proceedings of the IEEE International Conference on Robotics and Automation (ICRA) (2018): 1–8.
5. Lafmejani, A. S., Masouleh, M. T., and Kalhor, A. *Trajectory Tracking Control of a Pneumatically Actuated 6-DOF Gough–Stewart Parallel Robot Using Backstepping-Sliding Mode Controller and Geometry-Based Quasi Forward Kinematic Method*. Robotics and Computer-Integrated Manufacturing, 54 (2018): 96–114.
6. Schulz, S., Seibel, A., and Schlattmann, J. *Solution for the Direct Kinematics Problem of the General Stewart-Gough Platform by Using Only Linear Actuators' Orientations*. Advances in Robot Kinematics, 16 (2019): 241–250.
7. Lenarcic, J., and Parenti-Castelli, V. (Eds.). *Advances in Robot Kinematics*, Vol. 8. Springer (2018): 1–320.
8. Gallardo, J., and Alcaraz, L. A. *Kinematics of the Gough-Stewart Platform Using the Newton-Homotopy Method*. IEEE Latin America Transactions, 16(12) (2018): 2850–2856.
9. Markou, A. A., Elmas, S., and Filz, G. H. *Revisiting Stewart–Gough Platform Applications: A Kinematic Pavilion*. Engineering Structures, 249 (2021): 113304–113314.
10. Petrescu, R. V., et al. *Inverse Kinematics of a Stewart Platform*. Journal of Mechatronics and Robotics, 2(1) (2018): 45–59.
11. Morán, E. S., et al. *Design of a Spatial Disorientation Simulator Using a Modified Stewart-Gough Platform*. Proceedings of the IEEE Third Ecuador Technical Chapters Meeting (ETCM) (2018): 1–6.
12. Pfurner, M., Schröcker, H.-P., and Husty, M. *Path Planning in Kinematic Image Space Without the Study Condition*. Advances in Robot Kinematics 2016, Springer (2018): 285–294.
13. McCann, C. M., and Dollar, A. M. *Analysis and Dimensional Synthesis of a Robotic Hand Based on the Stewart-Gough Platform*. Proceedings of the International Design Engineering Technical Conferences and Computers and Information in Engineering Conference, 51807 (2018): 1–12.
14. Beiki, M. R. E., and Irani-Rahaghi, M. *Optimal Trajectory Planning of a Six DOF Parallel Stewart Manipulator*. Proceedings of the 6th RSI International Conference on Robotics and Mechatronics (ICRoM), IEEE (2018): 1–8.
15. Alwan, H. M., and Sarhan, R. A. *Modeling of Gough Stewart Robot Manipulator Inverse Kinematics by Using MSC ADAMS Software*. Journal of University of Babylon for Engineering Sciences, 26(6) (2018): 266–281.
16. Pedrammehr, S., et al. *Dynamic Analysis of Hexarot: Axis-Symmetric Parallel Manipulator*. Robotica, 36(2) (2018): 225–240.
17. Zubizarreta, A., et al. *Real-Time Direct Kinematic Problem Computation of the 3PRS Robot Using Neural Networks*. Neurocomputing, 271 (2018): 104–114.